NANO LETTERS
Letter
Cite This: Nano Lett. 2018, 18, 1814−1818
pubs.acs.org/NanoLett

Nanoladder Cantilevers Made from Diamond and Silicon

M. Héritier,[†] A. Eichler,*[,†] Y. Pan,[‡] U. Grob,[†] I. Shorubalko,[¶] M. D. Krass,[†] Y. Tao,*[,‡] and C. L. Degen*[,†]

[†]Department of Physics, ETH Zurich, Otto Stern Weg 1, 8093 Zurich, Switzerland
[‡]Rowland Institute at Harvard, 100 Edwin H. Land Boulevard, Cambridge, Massachusetts 02142, United States
[¶]Swiss Federal Laboratories for Materials Science and Technology EMPA, Uberlandstrasse 129, 8600 Duebendorf, Switzerland

Supporting Information

ABSTRACT: We present a "nanoladder" geometry that minimizes the mechanical dissipation of ultrasensitive cantilevers. A nanoladder cantilever consists of a lithographically patterned scaffold of rails and rungs with feature size ∼100 nm. Compared to a rectangular beam of the same dimensions, the mass and spring constant of a nanoladder are each reduced by roughly 2 orders of magnitude. We demonstrate a low force noise of 158^{+62}_{-42} zN and 190^{+42}_{-33} zN in a 1 Hz bandwidth for devices made from silicon and diamond, respectively, measured at temperatures between 100−150 mK. As opposed to bottom-up mechanical resonators like nanowires or nanotubes, nanoladder cantilevers can be batch-fabricated using standard lithography, which is a critical factor for applications in scanning force microscopy.

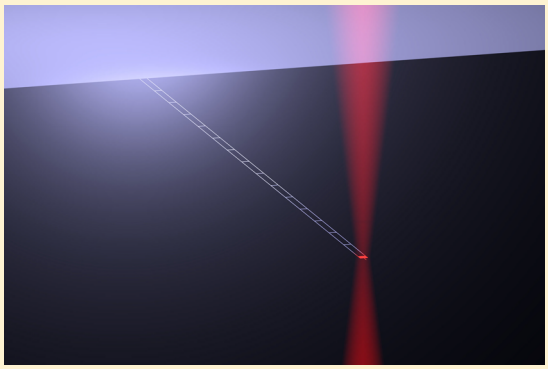

KEYWORDS: *Nanomechanics, force sensor, cantilever, scanning probe microscopy, diamond, silicon*

Nanomechanical sensors have emerged as powerful tools for the detection of minute masses[1−6] and forces,[7−14] opening avenues into nanobiology, chemistry, and solid state physics.[15−23] Similar to the atomic force microscope,[24] which was one of the key enabling instruments for the rise of nanotechnology, new generations of nanomechanical sensors will be instrumental in carrying industry to a new level of miniaturization and material control. Bottom-up fabricated nanoresonators based on individual, doubly clamped carbon nanotubes have recently demonstrated a mass sensitivity corresponding to a single hydrogen atom and a force resolution in the zeptonewton range.[4,11] A similar level of sensitivity has been achieved with untethered resonators like single trapped ions[25] and optically levitated nanoparticles.[26] However, the practical application of bottom-up sensors has so far been limited because they are difficult to implement in a scanning probe apparatus and are in many cases subject to large variations in quality, size, and geometry.

Top-down fabricated nanoresonators have remained the preferred devices for sensitive force measurements. They can be supplied in large numbers with small device-to-device variations, can take advantage of a wide range of substrate materials and also be geometry-tailored for specific applications. This makes top-down devices comparatively cheap and reliable. Among them, singly clamped cantilever beams form a particularly useful and versatile class of nanomechanical sensors due to their suitability for scanning probe experiments, such as atomic force microscopy (AFM),[24] magnetic force microscopy (MFM)[27] and magnetic resonance force microscopy (MRFM).[28,29] Owing to the limited spatial resolution of top-down lithography, however, the sensitivity of cantilever beams has trailed behind that of bottom-up devices. Current record sensitivities are on the order of $500 - 800\mathrm{zN}/\sqrt{\mathrm{Hz}}$ for devices made from low-dissipation materials including silicon[7] and diamond.[30]

The sensitivity of nanomechanical detectors is ultimately limited by thermomechanical force noise. In the absence of other noise sources, the minimum measurable force is given by $F_{\mathrm{th}} = (4\gamma k_{\mathrm{B}} T B)^{1/2}$, where γ describes the resonator dissipation, $k_{\mathrm{B}}T$ is the thermal energy, and B the measurement bandwidth.[31] Apart from reducing the operation temperature, the only means for reducing the force noise is through a reduction of the resonator dissipation $\gamma = \sqrt{km}/Q$. This translates into (i) combining a low spring constant k with (ii) a small effective mass m and (iii) employing a material that supports a high mechanical quality factor Q. Intuitively, both the spring constant and mass can be reduced by decreasing the cross section of the cantilever while maintaining the beam length.

In this Letter, we introduce a "nanoladder" geometry to reduce the force noise of top-down, batch produced ultrasensitive cantilevers. The nanoladder cantilever consists of two parallel wires joined by struts along their length (see Figure 1). The resulting structure maximizes stability along the transverse and longitudinal directions while minimizing the motional mass

Received: November 29, 2017
Revised: January 19, 2018
Published: February 7, 2018

DOI: 10.1021/acs.nanolett.7b05035
Nano Lett. 2018, 18, 1814−1818

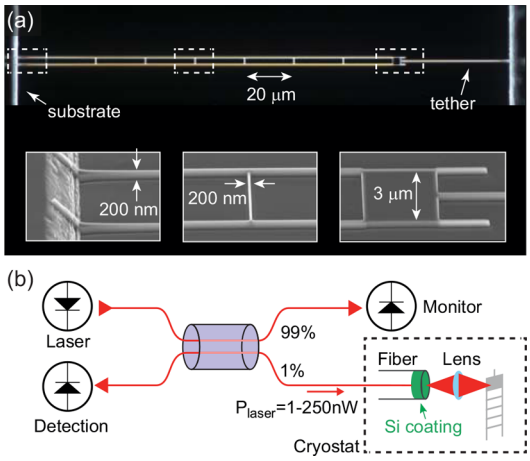

Figure 1. Nanoladder design and interferometric detection. (a) Optical micrograph of a 150 μm long diamond nanoladder device. The nanoladder consists of two parallel nanowires (length L, width w, height t) that are connected by rungs every 20 μm. Insets show magnified electron micrographs of the base, middle and tip regions of the device. A paddle located near the tip of the ladder allows for optical readout of the cantilever vibration. Devices fabricated for this study used $t \approx w$ = 100 to 300 nm and L = 100 to 300 μm. (b) Schematic of the nanowatt fiber-optic interferometer used for displacement detection.[7,33]

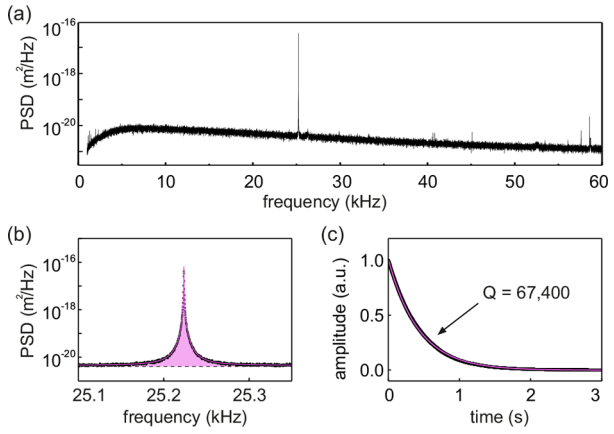

Figure 2. Characterization of a diamond nanoladder cantilever. (a) Power spectral density (PSD) of the cantilever displacement measured at room temperature. (b) PSD of the fundamental mode at f_c = 25.22 kHz. The shaded area corresponds to x^2_{rms}. The baseline reflects the displacement noise of the interferometer. (c) Ring-down experiment used to determine the Q-factor at room temperature (average over 100 ring-downs).

and spring constant of the sensing mode, and therefore combines the sensitivity of a nanowire detector with the rigidity of a cantilever beam. We experimentally demonstrate the performance of the nanoladder cantilever by achieving a force noise of 158zN/$\sqrt{\text{Hz}}$ at 108 mK.

We implemented the nanoladder design using diamond and silicon as resonator materials. Diamond devices were patterned by electron beam lithography onto a polished 20 μm thick single crystal membrane and released by inductively coupled plasma (ICP) etching from the backside.[30,32] Silicon devices used a low-conductivity SOI wafer and a vapor hydrofluoric acid (HF) etching process for device formation (see SI). In order to protect the fragile nanoladder structure during the final release, most of the cantilevers were tethered to the opposite support substrate (see Figure 1). The tether was cut postrelease by a focused helium ion beam (diamond devices) or mechanically with a manual micromanipulator stage (silicon devices). Optical and scanning electron micrographs of a finished diamond device are shown in Figure 1a; further images are provided in the SI.

We characterized the nanoladder cantilevers in a custom-built force microscope operating inside the vacuum chamber of a dilution refrigerator (Leiden CF450) with a minimum stage temperature of approximately 80 mK.[30] The microscope stage was suspended on springs to eliminate environmental vibrations. The subnanometer vibrations of the cantilevers were measured by a fiber-optic interferometer operating at a wavelength of 1550 nm (Figure 1b).[33] Only a few percent of the light incident at the cantilever were typically reflected back into the fiber because of the small size of the mirror paddle, and because the interferometer wavelength was not well matched to the cantilever thickness.[7,34]

In a first step, we measured the vibrational noise spectrum at room temperature (Figure 2a). The spectrum was dominated by a sharp signal peak at the frequency f_c of the fundamental mechanical mode, reflecting the thermomechanical motion of the cantilever. The higher order modes appeared at much larger frequencies (see SI), as expected from the high transverse and longitudinal stiffness of the nanoladder. To determine the spring constant k and effective mass m of the fundamental mode, we computed the mean square displacement x^2_{rms} by integrating the signal peak of the power spectral density (PSD) after subtracting the background (Figure 2b). In thermal equilibrium, the mean square displacement is linked to the spring constant by the equipartition theorem, $\frac{1}{2}kx^2_{rms} = \frac{1}{2}k_BT$, where T is the noise temperature of the resonant mode.[7] By performing this measurement at room temperature (T = 295 K) we could calibrate both the spring constant, $k = k_BT/x^2_{rms}$, and the effective mass, $m = k/(2\pi f_c)^2$. The quality factor Q was determined via the decay time constant $\tau = Q/(\pi f_c)$ of a separate ringdown measurement (Figure 2c). We found that the ring-down method and a fit to the spectral density gave similar values for the Q-factor, indicating that spectral diffusion is negligible.

Table 1 compares the mechanical properties of a diamond and a silicon nanoladder to state-of-the-art ultrasensitive cantilever beams (refs 7 and 35.). We find that the nanoladder devices have 50−400 times lower mass and are 40−600 times softer than their rectangular beam counterparts. Ideally, the nanoladder design should therefore allow for a reduction of the mechanical dissipation $\gamma = \sqrt{km}/Q$ by roughly 2 orders of magnitude. However, since the nanoladders also exhibit a significantly lower Q-factor than the corresponding rectangular beam devices, the reduction in mechanical dissipation is effectively about a factor of 15. The reduction in the Q-factor is probably related to the enhanced surface-to-volume ratio and to sidewall roughness, and will be the subject of a future study.

We now turn to the main result of this work, a measurement of the force noise of nanoladder cantilevers at cryogenic temperatures. For this purpose, the devices were cooled down to the base temperature of the dilution refrigerator. Below ~1 K, we observed that the mode temperature T of the cantilevers was higher than the stage temperature T_{stage} due to laser absorption at the paddle. To study the cantilever noise as a function of temperature, we therefore kept the stage temper-

DOI: 10.1021/acs.nanolett.7b05035
Nano Lett. 2018, 18, 1814−1818

Table 1. Mechanical Properties of Nanoladder Cantilevers and Corresponding Rectangular Beam Cantilevers[a]

device	f_c (kHz)	m (pg)	k (μN/m)	Q^b	γ (pg/s)	reference
nanoladder (diamond)	25.22	4.1 ± 0.6	110 ± 10	162,000	3.7	this work
rectangular beam (diamond)	32.14	1,600	67,000	6,000,000	55	Tao et al.[30]
nanoladder (silicon)	5.52	5.5 ± 1.3	6.5 ± 1.6	45,000	4.2	this work
rectangular beam (silicon)	4.98	270	260	150,000	55	Mamin et al.[7]

[a]Data for the diamond cantilever are for the device shown in Figure 1. A total of five diamond and two silicon devices were investigated (see SI). [b]Reported Q-factors represent the highest measured values at milliKelvin temperatures.

ature constant ($T_{stage} \sim 80$ mK) and varied the power P_{laser} of the laser light injected into the interferometer arm (see Figure 1b).

Figure 3a shows displacement spectra for the diamond cantilever as a function of P_{laser}. For each spectrum, we

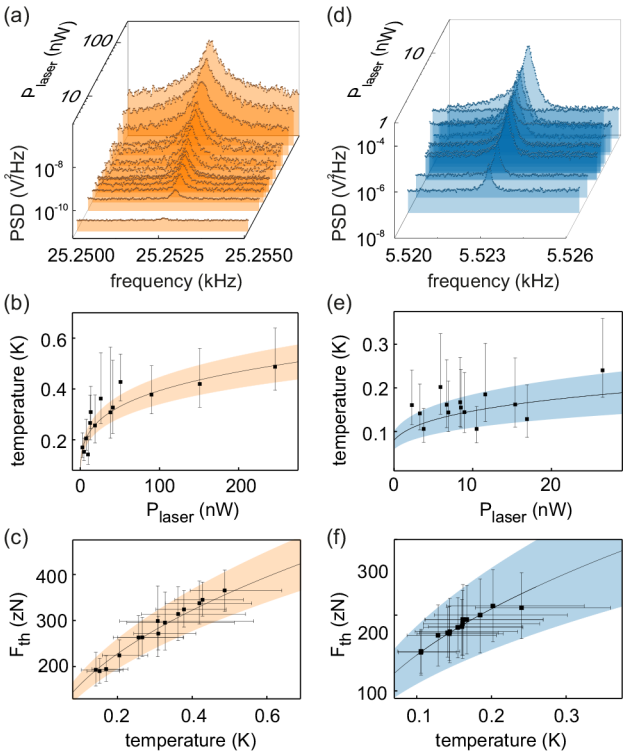

Figure 3. Characterization of nanoladder cantilevers at cryogenic temperatures. (a) Diamond device: thermal displacement PSD as a function of interferometer laser power. (b) Mode temperature as a function of interferometer laser power. (c) Thermal force noise (in a 1 Hz bandwidth) as a function of mode temperature. (d–f) Corresponding data for the silicon device. Error bars reflect the fit error and shaded areas indicates calibration uncertainty in the resonator mass (see SI). (Displacement PSD is given in units of V^2/Hz because the displacement sensitivity varied between measurements.)

calculated the mode temperature $T = mx_{rms}^2(2\pi f_c)^2/k_B$ by integrating the spectrum (after baseline subtraction) and using the known mass from the room temperature calibration measurement. The mode temperature roughly followed $T = (\epsilon P_{laser} + T_{stage}^4)^{1/4}$ as the laser power was reduced from P_{laser} = 250 nW to 1 nW, as expected from the thermal conductivity of diamond at low temperatures[30] [lines in Figure 3b,e]. The quality factor concurrently increased from Q = 131,000 to 162,000 (see SI). At the lowest temperature of $T \sim 140$ mK, the force noise reached a value of $F_{th} = 190^{+42}_{-33}$ zN in bandwidth B = 1 Hz. Note that because the experimenter also sees detector noise in addition to the force noise, the value for the force sensitivity is slightly higher, $F_{min} = 340^{+75}_{-59}$ zN (see SI). The dominant error in the force resolution is the calibration error of the cantilever displacement, which leads to an uncertainty in the estimate of the resonator mass (see SI and shaded areas in Figure 3).

Figure 3d–f shows the corresponding data for the silicon devices. Here, the minimum force noise is $F_{th} = 158^{+62}_{-42}$ zN and the force sensitivity is $F_{min} = 188^{+70}_{-48}$ zN at a mode temperature of $T \sim 110$ mK, almost identical to the diamond cantilever. These results demonstrate that the nanoladder design provides a generic improvement of the force noise independent of the resonator material.

Table 2 compares the force sensitivities of the nanoladder cantilevers to the cantilever beams of ref 7 and 30. Clearly, the

Table 2. Reported Sensitivities in Bandwidth B = 1 Hz for Ultrasensitive Cantilevers[a]

		F_{th} (aN)			
geometry	material	300 K	3 K[b]	100 mK	reference
nanoladder	diamond	13	1.1	0.19	this work
nanoladder	silicon	15	1.2	0.16	this work
singly clamped beam	diamond	115	6.0	0.54	Tao et al.[30]
singly clamped beam	silicon		4.7	0.82	Mamin et al.[7]
nanowire	silicon		1.5		Nichol et al.[22]
nanowire	GaAs/AlGaAs		5		Rossi et al.[36]
membrane	Si_3N_4	19.5			Reinhard et al.[13]
membrane	Si_3N_4	(10)[c]			Norte et al.[37]

[a]Prospective nanowire and membrane devices are included for reference. [b]Temperatures vary between 1 and 8 K. [c]Calculated (not measured).

nanoladder design provides a significant improvement compared to standard cantilever beams. In fact, to the best of our knowledge our experiments observed the lowest force noise that has been reported for a cantilever device. The nanoladder devices also equal or surpass the sensitivities offered by other prospective geometries considered for force microscopy, such as singly clamped nanowires[22,36] or two-dimensional membranes,[13,37] regardless of the experimental temperature. The sensitivity of the nanoladder devices could be further improved by lowering the mode temperature, which requires a suppression of the laser heating. This can be achieved by relatively simple means. A higher reflectivity of the cantilever mirror paddle, for example, will at the same time increase the signal amplitude and decrease the effect of absorptive heating, leading to lower mode temperatures. For this purpose, future generations of nanoladder cantilevers might be equipped with a

DOI: 10.1021/acs.nanolett.7b05035
Nano Lett. 2018, 18, 1814–1818

highly reflective mirror on the paddle.[38] It may also be possible to further improve the sensitivity by reducing the intrinsic dissipation of the devices, for example, by applying a chemical surface treatment,[35] reducing sidewall roughness, or by adopting phonon bandgap engineering ideas from optomechanical membranes.[39,40]

Looking forward, the nanoladder cantilever design can enable a significant step ahead in the mechanical detection of weak magnetic signals, such as those produced by nuclear or electronic spins in the context of magnetic resonance force microscopy.[29] For instance, the force generated on a single proton magnetic moment ($\mu = 1.4 \times 10^{-26}$ Am) by the field gradient of a strong nearby nanomagnet ($G = 2.8 \times 10^{7}$ T/m, ref 41) is $F = \mu G = 400$ zN, which is more than two times larger than the sensitivity limit (in a 1 Hz bandwidth) achieved in this work. It is therefore conceivable that nanoladder cantilevers will pave the way toward single nuclear spin detection, which is an important prerequisite for the three-dimensional magnetic resonance imaging of individual molecules with atomic resolution.[16,42] Diamond nanoladders with low dissipation are also of interest to ongoing efforts in optomechanics to exploit the excellent photonic properties of the material and its unique intrinsic lattice defects.[43]

■ ASSOCIATED CONTENT

Supporting Information

The Supporting Information is available free of charge on the ACS Publications Web site. The Supporting Information is available free of charge on the ACS Publications website at DOI: 10.1021/acs.nanolett.7b05035.

Device fabrication, characterization of further devices, finite element modeling, quality factor study, and estimation of mode temperature and force noise (PDF)

■ AUTHOR INFORMATION

Corresponding Authors

*E-mail: eichlera@phys.ethz.ch.
*E-mail: tao@rowland.harvard.edu.
*E-mail: degenc@ethz.ch.

ORCID

A. Eichler: 0000-0001-6757-3442
C. L. Degen: 0000-0003-2432-4301

Notes

The authors declare no competing financial interest.

■ ACKNOWLEDGMENTS

The authors thank Christoph Keck for experimental assistance. This work has been supported by the ERC through Starting Grant 309301, by the European Commission through the FP7-611143 DIADEMS programme, by the Swiss NSF through the NCCR QSIT, and by the ETH Research Grant ETH-03 16-1. Y.P. and Y.T. acknowledge funding from a Rowland Fellowship. I.S. is thankful to Empa for financial support and to Swiss National Science Foundation for support in equipment procurement (REquip 206021_133823).

■ REFERENCES

(1) Ekinci, K. L.; Huang, X. M. H.; Roukes, M. L. *Appl. Phys. Lett.* **2004**, *84*, 4469−4471.
(2) Chiu, H.-Y.; Hung, P.; Postma, H. W. C.; Bockrath, M. *Nano Lett.* **2008**, *8*, 4342−4346.
(3) Naik, A. K.; Hanay, M. S.; Hiebert, W. K.; Feng, X. L.; Roukes, M. L. *Nat. Nanotechnol.* **2009**, *4*, 445−449.
(4) Chaste, J.; Eichler, A.; Moser, J.; Ceballos, G.; Rurali, R.; Bachtold, A. *Nat. Nanotechnol.* **2012**, *7*, 301−304.
(5) Larsen, T.; Schmid, S.; Villanueva, L. G.; Boisen, A. *ACS Nano* **2013**, *7*, 6188−6193.
(6) Gil-Santos, E.; Baker, C.; Nguyen, D. T.; Hease, W.; Gomez, C.; Lemaître, A.; Ducci, S.; Leo, G.; Favero, I. *Nat. Nanotechnol.* **2015**, *10*, 810−816.
(7) Mamin, H. J.; Rugar, D. *Appl. Phys. Lett.* **2001**, *79*, 3358−3360.
(8) Arlett, J. L.; Maloney, J. R.; Gudlewski, B.; Muluneh, M.; Roukes, M. L. *Nano Lett.* **2006**, *6*, 1000−1006.
(9) Teufel, J. D.; Donner, T.; Castellanos-Beltran, M. A.; Harlow, J. W.; Lehnert, K. W. *Nat. Nanotechnol.* **2009**, *4*, 820−823.
(10) Gavartin, E.; Verlot, P.; Kippenberg, T. J. *Nat. Nanotechnol.* **2012**, *7*, 509−514.
(11) Moser, J.; Guettinger, J.; Eichler, A.; Esplandiu, M. J.; Liu, D. E.; Dykman, M. I.; Bachtold, A. *Nat. Nanotechnol.* **2013**, *8*, 493−496.
(12) Weber, P.; Güttinger, J.; Noury, A.; Vergara-Cruz, J.; Bachtold, A. *Nat. Commun.* **2016**, *7*, 12496.
(13) Reinhardt, C.; Müller, T.; Bourassa, A.; Sankey, J. C. *Phys. Rev. X* **2016**, *6*, 021001.
(14) de Lépinay, L. M.; Pigeau, B.; Besga, B.; Vincent, P.; Poncharal, P.; Arcizet, O. *Nat. Nanotechnol.* **2016**, *12*, 156−162.
(15) Rugar, D.; Budakian, R.; Mamin, H. J.; Chui, B. W. *Nature* **2004**, *430*, 329−332.
(16) Degen, C. L.; Poggio, M.; Mamin, H. J.; Rettner, C. T.; Rugar, D. *Proc. Natl. Acad. Sci. U. S. A.* **2009**, *106*, 1313−1317.
(17) Bleszynski-Jayich, A. C.; Shanks, W. E.; Peaudecerf, B.; Ginossar, E.; von Oppen, F.; Glazman, L.; Harris, J. G. E. *Science* **2009**, *326*, 272.
(18) Wang, Z.; Wei, J.; Morse, P.; Dash, J. G.; Vilches, O. E.; Cobden, D. H. *Science* **2010**, *327*, 552.
(19) Hanay, M. S.; Kelber, S.; Naik, A. K.; Chi, D.; Hentz, S.; Bullard, E. C.; Colinet, E.; Duraffourg, L.; Roukes, M. L. *Nat. Nanotechnol.* **2012**, *7*, 602−608.
(20) Olcum, S.; Cermak, N.; Wasserman, S. C.; Christine, K. S.; Atsumi, H.; Payer, K. R.; Shen, W.; Lee, J.; Belcher, A. M.; Bhatia, S. N.; Manalis, S. R. *Proc. Natl. Acad. Sci. U. S. A.* **2014**, *111*, 1310−1315.
(21) Tavernarakis, A.; Chaste, J.; Eichler, A.; Ceballos, G.; Gordillo, M. C.; Boronat, J.; Bachtold, A. *Phys. Rev. Lett.* **2014**, *112*, 196103.
(22) Nichol, J. M.; Hemesath, E. R.; Lauhon, L. J.; Budakian, R. *Phys. Rev. B: Condens. Matter Mater. Phys.* **2012**, *85*, 054414.
(23) Payne, A.; Ambal, K.; Boehme, C.; Williams, C. C. *Phys. Rev. B: Condens. Matter Mater. Phys.* **2015**, *91*, 195433.
(24) Binnig, G.; Quate, C. F.; Gerber, C. *Phys. Rev. Lett.* **1986**, *56*, 930−933.
(25) Biercuk, M. J.; Uys, H.; Britton, J. W.; VanDevender, A. P.; Bollinger, J. J. *Nat. Nanotechnol.* **2010**, *5*, 646−650.
(26) Hempston, D.; Vovrosh, J.; Toros, M.; Winstone, G.; Rashid, M.; Ulbricht, H. *Appl. Phys. Lett.* **2017**, *111*, 133111.
(27) Rugar, D.; Mamin, H. J.; Guethner, P.; Lambert, S. E.; Stern, J. E.; McFadyen, I.; Yogi, T. *J. Appl. Phys.* **1990**, *68*, 1169−1183.
(28) Sidles, J. A.; Garbini, J. L.; Bruland, K. J.; Rugar, D.; Züger, O.; Hoen, S.; Yannoni, C. S. *Rev. Mod. Phys.* **1995**, *67*, 249.
(29) Poggio, M.; Degen, C. L. *Nanotechnology* **2010**, *21*, 342001.
(30) Tao, Y.; Boss, J.; Moores, B.; Degen, C. *Nat. Commun.* **2014**, *5*, 3638.
(31) Stowe, T. D.; Yasumura, K.; Kenny, T. W.; Botkin, D.; Wago, K.; Rugar, D. *Appl. Phys. Lett.* **1997**, *71*, 288−290.
(32) Tao, Y.; Degen, C. *Adv. Mater.* **2013**, *25*, 3962−3967.
(33) Rugar, D.; Mamin, H. J.; Guethner, P. *Appl. Phys. Lett.* **1989**, *55*, 2588−2590.
(34) Mulhern, P. J.; Hubbard, T.; Arnold, C. S.; Blackford, B. L.; Jericho, M. H. *Rev. Sci. Instrum.* **1991**, *62*, 1280−1284.
(35) Tao, Y.; Navaretti, P.; Hauert, R.; Grob, U.; Poggio, M.; Degen, C. L. *Nanotechnology* **2015**, *26*, 465501.
(36) Rossi, N.; Braakman, F. R.; Cadeddu, D.; Vasyukov, D.; Tutuncuoglu, G.; Fontcuberta i Morral, A.; Poggio, M. *Nat. Nanotechnol.* **2016**, *12*, 150.

DOI: 10.1021/acs.nanolett.7b05035
Nano Lett. 2018, 18, 1814−1818

(37) Norte, R. A.; Moura, J. P.; Gröblacher, S. *Phys. Rev. Lett.* **2016**, *116*, 147202.
(38) Kemiktarak, U.; Durand, M.; Metcalfe, M.; lawall, J. *New J. Phys.* **2012**, *14*, 125010.
(39) Yu, P.-L.; Cicak, K.; Kampel, N. S.; Tsaturyan, Y.; Purdy, T. P.; Simmonds, R. W.; Regal, C. A. *Appl. Phys. Lett.* **2014**, *104*, 023510.
(40) Tsaturyan, Y.; Barg, A.; Polzik, E. S.; Schliesser, A. *Nat. Nanotechnol.* **2017**, *12*, 776.
(41) Tao, Y.; Eichler, A.; Holzherr, T.; Degen, C. L. *Nat. Commun.* **2016**, *7*, 12714.
(42) Sidles, J. A. *Appl. Phys. Lett.* **1991**, *58*, 2854.
(43) Rabl, P.; Cappellaro, P.; Dutt, M. V. G.; Jiang, L.; Maze, J. R.; Lukin, M. D. *Phys. Rev. B: Condens. Matter Mater. Phys.* **2009**, *79*, 41302.

DOI: 10.1021/acs.nanolett.7b05035
Nano Lett. 2018, 18, 1814−1818